









Article

Bioaccumulation Patterns in Different Tissues of Twelve Species of Elasmobranchs from the Tyrrhenian and Ionian Sea (Calabria, Southern Italy)

Samira Gallo ^{1,†}, Francesco Luigi Leonetti ^{1,†}, Francesca Romana Reinero ², Primo Micarelli ^{2,3},
Luigi Passarelli ¹, Gianni Giglio ¹, Concetta Milazzo ¹, Sandra Imbrogno ¹, Donatella Barca ^{1,†},
Massimiliano Bottaro ^{4,5,†} and Emilio Sperone ^{1,*,†}

¹ Department of Biology, Ecology and Earth Science, University of Calabria, 87036 Rende, Italy; samira.gallo@unical.it (S.G.); francescoluigi.leonetti@unical.it (F.L.L.); passarelli_luigi@yahoo.it (L.P.); gianni.giglio@unical.it (G.G.); concetta.milazzo@unical.it (C.M.); sandra.imbrogno@unical.it (S.I.); donatella.barca@unical.it (D.B.)

² Istituto Scientifico Centro Studi Squali, 58024 Valpiana, Italy; frreinero@gmail.com (F.R.R.); primo.micarelli@gmail.com (P.M.)

³ Department of Physical Sciences, Earth, and Environment, University of Siena, 53100 Siena, Italy

⁴ Department of Integrative Marine Ecology, Genoa Marine Centre, Stazione Zoologica Anton Dohrn-Italian National Institute of Marine Biology, Ecology and Biotechnology, 16126 Genoa, Italy; massimiliano.bottaro@szn.it

⁵ Triton ETS—Marine Research and Conservation, 00195 Rome, Italy

* Correspondence: emilio.sperone@unical.it; Tel.: +39-0984492972

† These authors contributed equally to this work.

Abstract: Marine ecosystems are increasingly threatened by pollutants, including trace elements (TEs) such as heavy metals, which bioaccumulate and pose risks to both marine fauna and human health. Sharks and rays are particularly susceptible to metal uptake and retention, making them sentinel species for assessing environmental contamination. This study investigated the bioaccumulation of 16 TEs across 12 elasmobranch species sampled from the Ionian and Tyrrhenian coasts of Calabria, southern Italy, over an 11-year period. Muscle tissue was analyzed for all species, while additional comparisons among skin, muscle, and brain tissues were conducted for *Galeus melastomus*. Statistical analyses revealed significant variability in TE concentrations across trophic levels (TRLs), with higher levels observed in species occupying higher trophic positions. Positive correlations were noted for elements such as Al, Ba, and Se, while negative correlations were found for Co, Cu, Mn, and U, indicating species-specific metabolic adaptations. Tissue-specific analyses identified the skin as a primary site for TE accumulation, likely due to its barrier functions and external exposure. This study highlights the complex interplay of ecological, dietary, and physiological factors influencing TE bioaccumulation in elasmobranchs and emphasizes the need for further research to understand the implications for marine food webs and conservation strategies.

Keywords: elasmobranch; Mediterranean Sea; tissues; trace elements; trophic level



Academic Editors: Vincenzo Di Martino and Francesco Tiralongo

Received: 10 December 2024

Revised: 23 December 2024

Accepted: 1 January 2025

Published: 3 January 2025

Citation: Gallo, S.; Leonetti, F.L.; Reinero, F.R.; Micarelli, P.; Passarelli, L.; Giglio, G.; Milazzo, C.; Imbrogno, S.; Barca, D.; Bottaro, M.; et al. Bioaccumulation Patterns in Different Tissues of Twelve Species of Elasmobranchs from the Tyrrhenian and Ionian Sea (Calabria, Southern Italy). *Environments* **2025**, *12*, 12. <https://doi.org/10.3390/environments12010012>

Copyright: © 2025 by the authors. Licensee MDPI, Basel, Switzerland. This article is an open access article distributed under the terms and conditions of the Creative Commons Attribution (CC BY) license (<https://creativecommons.org/licenses/by/4.0/>).

1. Introduction

In recent decades, there has been a notable rise in the levels of pollutants within marine ecosystems. Among these pollutants, trace elements have been the focus of close monitoring due to their persistence, toxicity, and tendency to accumulate in organisms [1]. Metals, including heavy metals (highly toxic metals such as arsenic, cadmium, mercury, and lead),

are released into the environment through natural and/or anthropogenic processes and can negatively affect marine fauna and human health given their toxicity and environmental persistence [2–6]. The uptake and tissue concentration of these metals in marine organisms are influenced by environmental and species-specific biological factors as well as the chemical and physical form in which metals occur in the environment [7]. Recent studies have demonstrated that sharks and rays show increased susceptibility to metal uptake and biomagnification, as they efficiently incorporate these compounds very efficiently and eliminate them slowly [8–10]. While determining patterns of heavy metal concentrations in sharks is important from the perspective of human food safety, the impacts of heavy metal exposure on the well-being of wild sharks remain poorly understood [11]. Anatomy and life cycle features of Chondrichthyes can potentially affect the intake and retention of certain metals. Due to these traits and known species-specific life history parameters, these animals are often regarded as sentinel species for environmental contamination [12–14]. Some species have a vast home range, making it challenging to identify the source of contamination, while others have more restricted movements and can therefore provide more information on the contamination of a particular area [5,15–18]. In sharks, exposure and heavy metal toxicity are primarily driven by dietary uptake [19,20]. Overfishing in coastal zones leads top predators such as sharks towards searching for food at higher trophic levels, resulting in the bioaccumulation of metals in their tissues [21]. As diet is the main source of these contaminants, understanding the feeding ecology of these top predators is crucial for identifying potential pathways of metal transfer within marine food webs [22]. However, available data on this topic remain limited [2,23–25], and further research is required on a broader range of species.

This study aimed to compare bioaccumulation levels of trace elements across 12 different species of elasmobranchs, seven of which are classified in risk categories according to the last IUCN assessments [26]: *Centrophorus granulosus* (critically endangered—MED; endangered—global) *Dalatias licha* (vulnerable—global), *Galeorhinus galeus* (critically endangered—global), *Galeus melastomus* (least concern—global), *Hexanchus griseus* (near threatened—global), *Heptranchias perlo* (data deficient—MED; near threatened—global), *Isurus oxyrinchus* (critically endangered—MED; endangered—global), *Prionace glauca* (critically endangered—MED; near threatened—global), *Pteroplatytrygon violacea* (least concern—MED and global), *Squalus acanthias* (endangered—MED; vulnerable—global), *Scyliorhinus canicula* (least concern—MED and global), *Torpedo torpedo* (least concern—MED; vulnerable—global). This comparison aims to investigate (a) differences between species, (b) differences across various trophic levels, and (c) potential correlations between trophic level and the bioaccumulation of trace elements. Additionally, for one species (*Galeus melastomus*), the analysis will include a comparison of bioaccumulation in three different tissues to identify affinities for trace elements (TEs) and metabolic patterns.

2. Materials and Methods

2.1. Study Area and Sample Collection

Samples were collected from different localities along the Ionian and Tyrrhenian coasts of Calabria, in southern Italy (Figure 1). Calabria, together with Sicily and the Tunisian coast, divides the Mediterranean Sea into western and eastern parts: the Tyrrhenian side of Calabria lies in the western Mediterranean, while the Ionian side lies in the eastern Mediterranean [27].



Figure 1. Distribution of the sampling locations. The number shown inside the points represents the number of species coming from that area. The size of the points is proportional to the number of species.

The samples collected were obtained from specimens caught either as by-catch or acquired during stranding events and identified using the guidelines established by Ebert et al. [28]. The total number of samples was collected from 53 individuals, corresponding to different shark ($N = 10$) and ray ($N = 2$) species, over a period of 11 years (from 2010 to 2021); it is worth noting that some of the data concerning *G. melastomus* were extrapolated from our previous study [29,30]. Table 1 reports for each species the year of collection, the locality, the ecology, the trophic level, and the source. Muscle tissue was analyzed as the primary target for all species, while comparative analysis of different tissues (muscle, skin, and brain) was conducted only for one species (*Galeus melastomus*).

Due to the lack of complete morphometric data, which prevented their use as a grouping variable, results were categorized by trophic level (TRL) following the frameworks proposed by Cortès [31] and Jacobsen and Bennett [32], as detailed in Table 1. For species with n specimens > 1 , more extensive statistical analyses were performed, allowing interspecies comparisons among five selected species.

Table 1. Comprehensive dataset of analyzed specimens. This table shows the code assigned to each specimen along with its corresponding species. Additionally, it includes the trophic level (TRL), the ecological category (D for demersal, P for pelagic), the year in which the sample was acquired, the location of origin, whether the location falls within the Tyrrhenian or Ionian basin, and finally the origin of the specimen (“Stranded” or obtained after capture (either accidental or intentional) during “Fishing activity”). Samples extracted from the previous work by Gallo et al. [29] are marked with an asterisk (*).

Code	Species	TRL	Ecology	Year	Location	Basin	Source
#4	<i>C. granulatus</i>	4.1	D	2017	Paola (CS)	Tyrrhenian Sea	Stranded
#2	<i>D. licha</i>	4.1	D	2008	Vibo marina (VV)	Tyrrhenian Sea	Fishing activity
#13	<i>D. licha</i>	4.1	D	2008	Vibo marina (VV)	Tyrrhenian Sea	Fishing activity
#16	<i>D. licha</i>	4.1	D	2015	Schiavonea (CS)	Ionian Sea	Fishing activity
#23	<i>D. licha</i>	4.1	D	2014	Montepaone lido (CZ)	Ionian Sea	Fishing activity
#30	<i>D. licha</i>	4.1	D	2012	Crotone (KR)	Ionian Sea	Stranded
GG1	<i>G. galeus</i>	4.2	D	2013	Pellaro (RC)	Ionian Sea	Fishing activity
GMF1	<i>G. melastomus</i>	3.7	D	2010	Fiumefreddo Bruzio (CS)	Tyrrhenian Sea	Fishing activity
GMF2	<i>G. melastomus</i>	3.7	D	2010	Fiumefreddo Bruzio (CS)	Tyrrhenian Sea	Fishing activity
GMF3	<i>G. melastomus</i>	3.7	D	2010	Fiumefreddo Bruzio (CS)	Tyrrhenian Sea	Fishing activity
GMF4	<i>G. melastomus</i>	3.7	D	2010	Fiumefreddo Bruzio (CS)	Tyrrhenian Sea	Fishing activity
GMF5	<i>G. melastomus</i>	3.7	D	2010	Fiumefreddo Bruzio (CS)	Tyrrhenian Sea	Fishing activity
GM001	<i>G. melastomus</i> *	3.7	D	2020	Golfo di Sant’Eufemia (CZ)	Tyrrhenian Sea	Fishing activity
GM023	<i>G. melastomus</i> *	3.7	D	2021	Golfo di Sant’Eufemia (CZ)	Tyrrhenian Sea	Fishing activity
GM024	<i>G. melastomus</i> *	3.7	D	2021	Golfo di Sant’Eufemia (CZ)	Tyrrhenian Sea	Fishing activity
GM026	<i>G. melastomus</i> *	3.7	D	2021	Golfo di Sant’Eufemia (CZ)	Tyrrhenian Sea	Fishing activity
GM032	<i>G. melastomus</i> *	3.7	D	2021	Golfo di Sant’Eufemia (CZ)	Tyrrhenian Sea	Fishing activity
GM033	<i>G. melastomus</i> *	3.7	D	2021	Golfo di Sant’Eufemia (CZ)	Tyrrhenian Sea	Fishing activity
GM002	<i>G. melastomus</i> *	3.7	D	2020	Golfo di Sant’Eufemia (CZ)	Tyrrhenian Sea	Fishing activity
GM003	<i>G. melastomus</i> *	3.7	D	2020	Golfo di Sant’Eufemia (CZ)	Tyrrhenian Sea	Fishing activity
GM006	<i>G. melastomus</i> *	3.7	D	2020	Golfo di Sant’Eufemia (CZ)	Tyrrhenian Sea	Fishing activity
GM031	<i>G. melastomus</i> *	3.7	D	2021	Golfo di Sant’Eufemia (CZ)	Tyrrhenian Sea	Fishing activity
GM052	<i>G. melastomus</i> *	3.7	D	2021	Golfo di Sant’Eufemia (CZ)	Tyrrhenian Sea	Fishing activity
GM121	<i>G. melastomus</i> *	3.7	D	2021	Golfo di Taranto (CS)	Ionian Sea	Fishing activity

Table 1. Cont.

Code	Species	TRL	Ecology	Year	Location	Basin	Source
GM122	<i>G. melastomus</i> *	3.7	D	2021	Golfo di Taranto (CS)	Ionian Sea	Fishing activity
GM123	<i>G. melastomus</i> *	3.7	D	2021	Golfo di Taranto (CS)	Ionian Sea	Fishing activity
GM124	<i>G. melastomus</i> *	3.7	D	2021	Golfo di Taranto (CS)	Ionian Sea	Fishing activity
GM125	<i>G. melastomus</i> *	3.7	D	2021	Golfo di Taranto (CS)	Ionian Sea	Fishing activity
GM166	<i>G. melastomus</i> *	3.7	D	2021	Golfo di Taranto (CS)	Ionian Sea	Fishing activity
GM126	<i>G. melastomus</i> *	3.7	D	2021	Golfo di Taranto (CS)	Ionian Sea	Fishing activity
GM128	<i>G. melastomus</i> *	3.7	D	2021	Golfo di Taranto (CS)	Ionian Sea	Fishing activity
GM167	<i>G. melastomus</i> *	3.7	D	2021	Golfo di Taranto (CS)	Ionian Sea	Fishing activity
#5	<i>H. griseus</i>	4.3	D	2015	Crotone (KR)	Ionian Sea	Fishing activity
#25	<i>H. griseus</i>	4.3	D	2013	Torretta di Crucoli (KR)	Ionian Sea	Fishing activity
#26	<i>H. griseus</i>	4.3	D	2015	Crotone (KR)	Ionian Sea	Fishing activity
#28	<i>H. griseus</i>	4.3	D	2015	Corigliano Calabro (CS)	Ionian Sea	Stranded
HGF1	<i>H. griseus</i>	4.3	D	2012	Torretta di Crucoli (KR)	Ionian Sea	Fishing activity
HGF2	<i>H. griseus</i>	4.3	D	2016	Cetraro (CS)	Tyrrhenian Sea	Stranded
#8	<i>H. perlo</i>	4.2	D	2012	Bovalino (RC)	Ionian Sea	Stranded
#27	<i>I. oxyrinchus</i>	4.3	P	2012	Soverato (CZ)	Ionian Sea	Fishing activity
#6	<i>P. glauca</i>	4.1	P	2018	Schiavonea (CS)	Ionian Sea	Stranded
#20	<i>P. glauca</i>	4.1	P	2014	Bianco (RC)	Ionian Sea	Stranded
#21	<i>P. glauca</i>	4.1	P	2014	Villa San Giovanni (RC)	Tyrrhenian Sea	Stranded
#22	<i>P. glauca</i>	4.1	P	2014	Cirò marina (KR)	Ionian Sea	Fishing activity
#24	<i>P. glauca</i>	4.1	P	2013	Punta Alice (KR)	Ionian Sea	Stranded
#29	<i>P. glauca</i>	4.1	P	2015	Sibari (CS)	Ionian Sea	Stranded
#7	<i>P. violacea</i>	3.6	D	2013	Cirò marina (KR)	Ionian Sea	Fishing activity
#9	<i>S. acanthias</i>	3.9	D	2012	Cetraro (CS)	Tyrrhenian Sea	Fishing activity
#10	<i>S. acanthias</i>	3.9	D	2012	Cetraro (CS)	Tyrrhenian Sea	Fishing activity
#11	<i>S. acanthias</i>	3.9	D	2012	Cetraro (CS)	Tyrrhenian Sea	Fishing activity
#12	<i>S. acanthias</i>	3.9	D	2012	Cetraro (CS)	Tyrrhenian Sea	Fishing activity
SCF1	<i>S. canicula</i>	3.6	D	2010	Cetraro (CS)	Tyrrhenian Sea	Fishing activity
#15	<i>T. torpedo</i>	4.2	D	2011	Cetraro (CS)	Tyrrhenian Sea	Fishing activity

2.2. Trace Elements Analysis

Sixteen trace elements (TEs) were investigated using inductively coupled plasma mass spectrometry (ICP-MS; PerkinElmer/SCIEX, ELAN DRC-e). Before the analysis, the samples were processed following the protocol by De Donato et al. and Gallo et al. [29,30]. In brief, tissue samples are dissolved through acid digestion using ultrapure HNO₃, with the following proportions: 12 mL of acid are added per 0.1 g (dry weight) of tissue in proper vessels. After digestion, all samples are diluted to the same final volume of 100 mL using ultrapure water (UPW) and stored at 4 °C until ICP-MS analysis. During the drying phases, the tissue's water percentage was also measured (only for muscle), thus allowing the conversion of the dry weight values, returned by the ICP-MS, to wet weight (mg/Kg), using the equation of Gaion et al. [33]:

$$WW = DW \times (1 - WP)$$

where WW is the wet weight, DW is the dry weight, and WP is the water per-centage loss during the drying stage. The blank was prepared with ultra-pure water and ultrapure nitric acid (100 µL HNO₃:10 mL UPW). The percentage of water loss was calculated to be on average −71.2%.

The ICP-MS was calibrated using the ICP multi-element standard solution VI for ICP-MS (Merck). The accuracy of the method was evaluated using the Lobster Hepatopancreas (Tort-3; National Research Council Canada) as the certified reference material (CRM). The same preparation procedure was used on the CRM, and these solutions were used as unknown samples during the analytical sequence. During the analysis, the blank and the CRM were processed by the ICP-MS at the beginning and at the end and were also interspersed with every six samples (checking that the values were always in the norm and that the drift of the instrument did not affect the results obtained) [29]. The detection limit was set at three times the standard deviation of the blanks, and its value oscillated around 0.13 mg/kg.

2.3. Statistical Analysis

To enable more robust statistical assessments across all species, a classification criterion was developed to include species represented by only a single specimen, ensuring the applicability of inferential statistical tests. Statistical analyses were conducted using the Kruskal–Wallis test to compare differences across species, trophic levels, and tissue samples of *G. melastomus*, followed by Dunn’s post hoc test with Bonferroni correction to control for multiple comparisons. Additionally, the effect size was evaluated through the calculation of eta-squared (ϵ^2): values < 0,1 indicate “Small effect”, values between 0.1 and 0.6 stand for “Medium effect” and values > 0.6 stand for “Large effect”. To further investigate bioaccumulation trends in relation to trophic levels, Spearman’s rank correlation was employed to assess the strength and direction of these relationships.

3. Results and Discussion

3.1. Muscle Tissue

The analysis of muscle tissue involved the quantification of 16 TEs: Al, As, Ba, Bi, Co, Cr, Cu, Fe, Mn, Mo, Ni, Pb, Se, Sr, U, and Zn. The raw analytical data are provided in Table S1 (Supplementary Material). By quantitatively analyzing the raw results, it can be observed that—when comparing the outcomes obtained for species with a single specimen ($n = 1$) to the average values obtained for species with n specimens > 1—*P. violacea* (Ba, Cu, Fe, Mn, Se, Sr, and Zn) and *T. torpedo* (As, Cr, and Mo) more frequently exhibit the highest values. This might misleadingly suggest differences between sharks and batoids. However, since both species fall within the category of species with $n = 1$, the sample size is too small to confidently conclude that the differences follow taxonomic patterns. For this reason, it was decided to group the results based on trophic level (TRL) rather than species and to separately conduct species-specific analyses including only the five species with $n > 1$.

In Table 2, it is possible to see the results on which the species-specific analysis was based, including mean values, standard deviations, n specimens, and maximum concentrations for each TE. The highest concentrations were primarily observed in *H. griseus* and *D. licha*, which respectively accounted for 31% of the TEs analyzed (Figure 2). The consistently high TE levels found in these two species imply that, possibly due to their feeding strategies or metabolic processing, they are particularly prone to TE accumulation.

To compare the results obtained in the present study with the existing literature, a conversion from dry weight to wet weight was carried out (Table 3). Although the literature on both trace elements and elasmobranchs often focuses on only a few elements (primarily Hg) and few species, it was possible nonetheless to cross-reference some results for certain species. For instance, several scientific studies are available on the blue shark (*Prionace glauca*), the bluntnose sixgill shark (*Hexanchus griseus*), and the blackmouth catshark (*Galeus melastomus*).

Table 2. Concentration values for species-specific analysis. The following table reports the mean values, standard deviation, and number of samples (*n*) for each of the five species analyzed, for each trace element (TE). The last column shows the highest mean value obtained for that element. All values are expressed in ppm (mg/kg) and refer to dry weight (d.w.); bdl = below detection limit.

	<i>G. melastomus</i>			<i>D. licha</i>			<i>P. glauca</i>			<i>S. acanthias</i>			<i>H. griseus</i>			Max Value
	Mean	St. Dev.	<i>n</i>	Mean	St. Dev.	<i>n</i>	Mean	St. Dev.	<i>n</i>	Mean	St. Dev.	<i>n</i>	Mean	St. Dev.	<i>n</i>	
Al27	7.652	4.672	25	13.540	4.700	5	35.997	56.761	6	22.150	10.114	4	45.693	53.702	6	45.693
As75	118.714	35.833	25	91.166	62.984	5	76.130	55.327	6	85.630	21.468	4	80.710	53.134	6	118.714
Ba138	0.183	0.429	25	0.392	0.100	5	0.523	0.725	6	0.360	0.175	4	0.628	0.204	6	0.628
Bi209	0.007	0.007	25	0.026	0.012	5	0.022	0.004	6	0.023	0.004	4	0.023	0.004	6	0.026
Co59	0.044	0.019	25	0.024	0.010	5	0.047	0.022	6	0.038	0.008	4	0.033	0.008	6	0.047
Cr52	0.925	0.663	25	1.152	0.450	5	0.820	0.261	6	1.558	0.863	4	1.468	0.498	6	1.558
Cu63	1.959	1.829	25	0.850	0.130	5	1.400	0.690	6	1.098	0.323	4	1.015	0.148	6	1.959
Fe57	41.901	39.630	25	66.738	17.379	5	53.237	24.760	6	43.858	13.662	4	59.068	30.931	6	66.738
Mn55	0.986	0.438	25	0.836	0.232	5	0.747	0.411	6	0.780	0.168	4	0.945	0.411	6	0.986
Mo98	0.048	0.023	25	0.246	0.312	5	0.143	0.128	6	0.223	0.084	4	0.195	0.211	6	0.246
Ni60	1.991	1.177	25	6.242	4.056	5	3.817	2.636	6	7.188	4.541	4	13.180	3.856	6	13.180
Pb208	0.141	0.109	25	0.372	0.169	5	0.165	0.110	6	0.213	0.066	4	0.215	0.069	6	0.372
Se82	0.939	0.177	25	2.238	0.585	5	2.010	0.533	6	1.345	0.092	4	1.383	0.134	6	2.238
Sr88	2.513	0.953	25	4.044	1.183	5	4.092	1.602	6	6.853	0.329	4	4.823	0.954	6	6.853
U238	0.007	0.005	25	bdl	bdl	5	bdl	bdl	6	bdl	bdl	4	0.008	0.013	6	0.008
Zn64	21.529	5.847	25	29.322	9.602	5	37.890	19.714	6	26.710	7.853	4	48.370	16.910	6	48.370

SPECIES WITH HIGHEST VALUES

■ *G. melastomus* ■ *D. licha* ■ *P. glauca* ■ *S. acanthias* ■ *H. griseus*

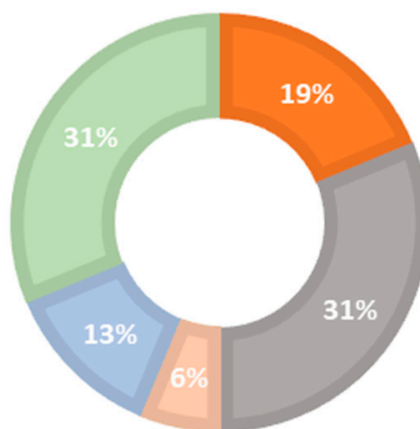


Figure 2. Concentration peaks in species-specific analysis. The chart shows, in percentage, how often (among the analyzed TEs) the different species recorded higher mean values compared to the others.

Table 3. Mean values conversion to wet weight. The following table reports the mean values expressed in ppm (mg/kg) and referred to wet weight (w.w.), for each of the five species analyzed, for each trace element (TE).

	<i>G. melastomus</i>	<i>D. licha</i>	<i>P. glauca</i>	<i>S. acanthias</i>	<i>H. griseus</i>
Al27	2.219	3.927	10.439	6.424	13.251
As75	34.427	26.438	22.078	24.833	23.406
Ba138	0.053	0.114	0.152	0.104	0.182
Bi209	0.002	0.008	0.006	0.007	0.007
Co59	0.013	0.007	0.014	0.011	0.009
Cr52	0.268	0.334	0.238	0.452	0.426
Cu63	0.568	0.247	0.406	0.318	0.294
Fe57	12.151	19.354	15.439	12.719	17.130
Mn55	0.286	0.242	0.217	0.226	0.274
Mo98	0.014	0.071	0.042	0.065	0.057
Ni60	0.577	1.810	1.107	2.084	3.822
Pb208	0.041	0.108	0.048	0.062	0.062
Se82	0.272	0.649	0.583	0.390	0.401
Sr88	0.729	1.173	1.187	1.987	1.399
U238	0.002	0.000	0.000	0.000	0.002
Zn64	6.243	8.503	10.988	7.746	14.027

For *Hexanchus griseus*, the values obtained in this study for most elements are consistent with those reported in previous studies [34–37], except for aluminum (Al), which is significantly higher than the levels reported for the Aegean Sea by Roubie et al. [34]. Similarly, nickel (Ni) concentrations exceed those documented by both Giovos et al. and Roubie et al. [34,37] for the Aegean Sea. Zinc (Zn) levels are also notably higher compared to the values reported by other authors [34,35,37].

For *Prionace glauca*, the existing literature is more extensive. Consequently, we focused on evaluating the main differences for some of the more debated elements. Regarding arsenic (As), the mean concentration (wet weight) obtained in this study is consistent with the findings of Roubie et al. [34] for the Aegean Sea but higher than the values they reported for the Ionian Sea. Our results also exceed those reported by Torres et al. [38] for the Azores, while being lower than those documented by Alves et al. [5] for the Atlantic.

Nickel (Ni) concentrations in our study are higher than those reported for the Atlantic Ocean [5], the NW Atlantic [39], and both the Aegean and Ionian Seas [34]. However, our values are lower than those reported for the Colima coast (Mexico) [40] and the English Channel [14].

For lead (Pb), our results are comparable to those reported for the NW Atlantic [39] and the Ionian Sea [34], higher than those from the English Channel [14], but lower than the values documented for the Colima coast [40], the Atlantic [5], and the Aegean Sea [34].

For *Galeus melastomus*, the mean concentrations of Pb and Ni found in this study are higher than those reported by Mille et al. [41] for the NW Mediterranean and the NE Atlantic. In contrast, our arsenic (As) and Pb concentrations are slightly lower than those reported by Gaion et al. [31] for the northern Tyrrhenian Sea.

The findings highlight significant geographical variability in heavy metal concentrations, likely influenced by local anthropogenic activities (e.g., industry, agriculture, maritime transport) and oceanographic conditions (e.g., currents, salinity, sediments).

The Kruskal–Wallis test revealed significant interspecies differences for 14 out of 16 TEs (Table S2), while the Dunn’s post hoc test identified pair-wise differences only in 10 of these TEs (Ba, Bi, Cr, Cu, Mo, Ni, Pb, Se, Sr, and U) (Figure 3). *G. melastomus* consistently displayed significant differences compared to other species. To assess potential bias due to

sample size (n), the effect size (ϵ^2) was computed; all TEs except Bi exhibited values < 0.6 , indicating low to moderate influence and confirming the reliability of the results.

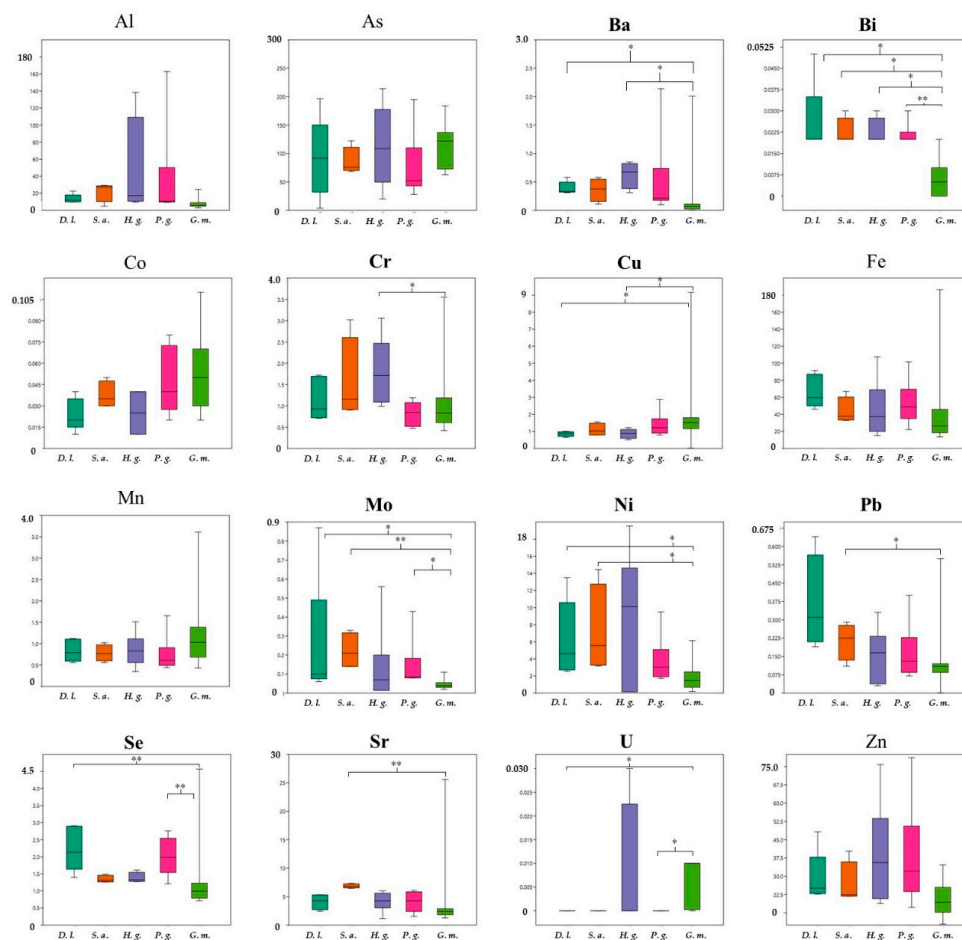


Figure 3. Species-specific comparison. Kruskal–Wallis and Dunn’s post hoc tests performed for five species with more than one individual. The figure includes box plots (with standard deviation) for 16 elements. Elements showing significant differences are highlighted in bold. The figure also shows the species that exhibited significant differences according to Bonferroni correction during Dunn’s post hoc test, as follows: $p \leq 0.05$ (*), $p \leq 0.001$ (**). On the X-axis, the species are represented with the following abbreviations: “D.l.” for *Dalatias licha*, “S.a.” for *Squalus acanthias*, “H.g.” for *Hexanchus griseus*, “P.g.” for *Prionace glauca*, and “G.m.” for *Galeus melastomus*. On the Y-axis, the concentration is reported relative to dry weight and expressed in ppm (mg/Kg).

These results emphasize the need for ongoing monitoring of contamination levels across species and regions to detect trends and evaluate the effectiveness of mitigation strategies. Further studies are warranted to understand the mechanisms of bioaccumulation and biomagnification in marine food webs.

Moving on to the data analysis based on trophic level, the Kruskal–Wallis test indicated statistically significant differences in 12 out of 16 elements among the six trophic levels (TRLs), with no significant variation detected for As, Cr, Mn, and Pb (Figure 4 and Table S3). Nine TEs exhibited consistent significant differences specifically between TRL 3.7 (represented by *G. melastomus*) and TRL 4.1 (encompassing *P. glauca*, *C. granulosus*, and *D. licha*). Notably, TRL 3.7 demonstrated statistically significant differentiation across all 9 elements examined. The ϵ^2 showed that only Bi exhibited values > 0.6 , indicating an influence of the size. [34,35,37].

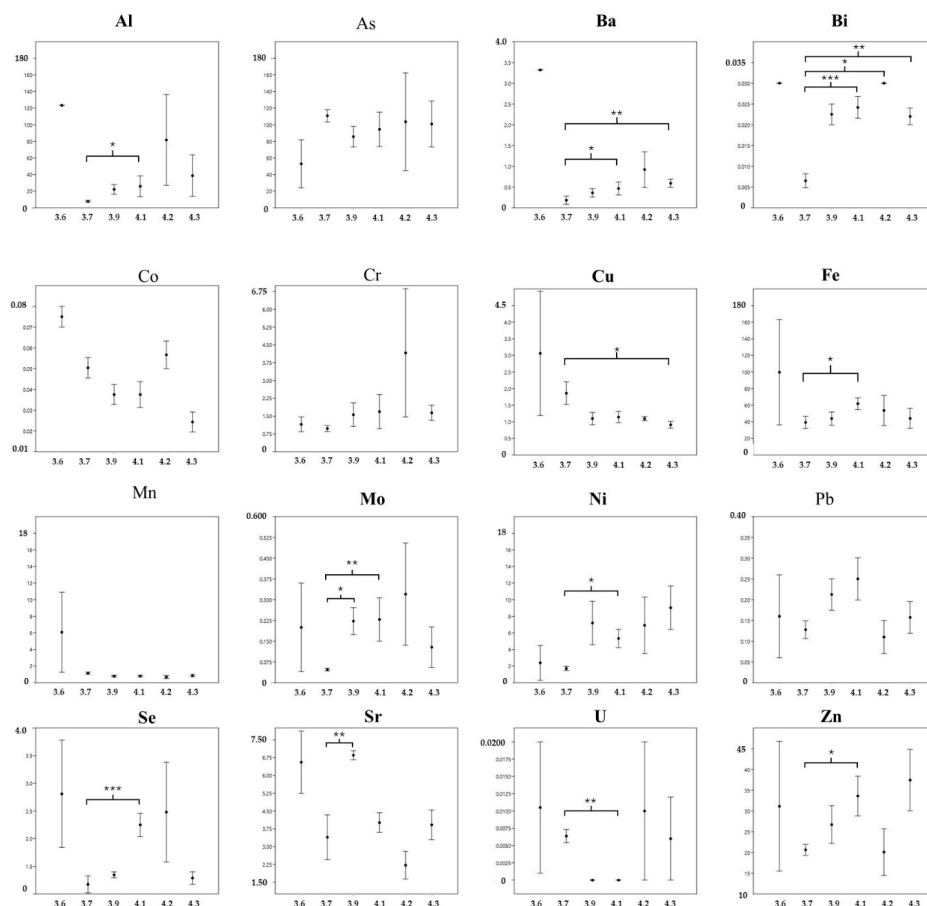


Figure 4. Trophic level comparison. Kruskal–Wallis and Dunn’s post hoc tests performed for trophic levels. The figure includes mean and whisker plots (with standard error) for all 16 elements. Elements showing significant differences are highlighted in bold. The figure also shows the TRLs that exhibited significant differences according to Bonferroni correction during Dunn’s post hoc test, as follows: $p \leq 0.05$ (*), $p \leq 0.001$ (**), $p \leq 0.0001$ (***) . On the X-axis, the different trophic levels are represented, while on the Y-axis, the concentration is reported relative to dry weight and expressed in ppm (mg/Kg).

To elucidate the relationship between TE concentrations and TRLs, Spearman’s rank correlation analysis was performed (Figure 5). Statistically significant correlations were identified for 12 of the 16 elements: positive correlations (indicating an increase in TE concentration with ascending trophic level) were observed for 8 elements (Al, Ba, Bi, Cr, Mo, Ni, Se, and Zn), while 4 elements (Co, Cu, Mn, and U) exhibited negative correlations (indicating a decrease in TE concentration with increasing TRL).

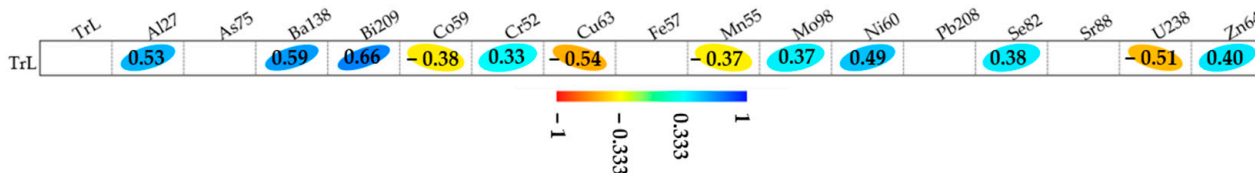


Figure 5. Spearman’s correlation about trophic levels/TEs concentration. The image displays ellipses only for elements where the correlation (positive or negative) showed statistical significance ($p < 0.05$). The color of the ellipses, as indicated in the legend, ranges from blue (slope coefficient equal to 1) to red (slope coefficient equal to -1). The value displayed at the center of each ellipse represents the coefficient observed.

Elements As, Fe, Pb, and Sr appeared to show no correlation with TRL, which may suggest that their bioaccumulation is not strongly linked to trophic level or dietary intake [42]. The positive correlations identified for elements such as Al, Ba, and Se could indicate that diet plays a significant role in the bioaccumulation of these TEs. Conversely, the negative correlations observed for Co, Cu, Mn, and U might imply that mechanisms such as excretion or metabolic regulation help mitigate TE concentrations as trophic levels increase [7,43]. This potential trend in TE metabolism could reflect species-specific adaptations aimed at reducing toxicity or managing essential element concentrations.

3.2. Comparison Among Tissues

A comparative analysis of tissues encompassing 15 TEs (As, Co, Cd, Cr, Cu, Fe, Mn, Mo, Ni, Pb, Se, Sn, Sr, U, and Zn) was conducted on *G. melastomus*. Mean values, standard deviations, *n* samples, and maximum values are presented in Table 4, while the raw results are listed in Table S4. Notably, the skin showed the highest mean concentrations for the majority of TEs (67%), suggesting its significant role in TE accumulation, possibly due to its direct exposure to the external environment and its involvement in barrier functions. The brain followed with elevated concentrations for 27% of the elements, indicating that certain TEs may preferentially accumulate in neural tissues, potentially due to either their essential roles in neurological processes (e.g., Cu) or to antagonist effects and increased binding affinity (e.g., Cd) or limited capacity for detoxification.

Table 4. Concentration values for tissues analysis. Mean values, standard deviation, and number of samples (*n*) for each tissue analyzed, for each trace element (TE). The last column shows the highest mean values. All values are expressed in ppm (mg/kg) and refer to dry weight (d.w.).

	Muscle			Skin			Brain			Max Value
	Mean	St. Dev.	<i>n</i>	Mean	St. Dev.	<i>n</i>	Mean	St. Dev.	<i>n</i>	
As75	79.350	15.082	5	41.420	20.212	3	75.325	25.255	2	79.350
Cd112	0.054	0.034	5	0.120	0.099	3	0.150	0.060	2	0.150
Co59	0.076	0.026	5	0.227	0.021	3	0.220	0.040	2	0.227
Cr52	1.176	0.358	5	1.297	0.333	3	1.380	0.510	2	1.380
Cu63	1.466	0.583	5	2.593	0.827	3	10.645	0.245	2	10.645
Fe57	28.794	17.084	5	359.057	71.277	3	67.950	14.520	2	359.057
Mn55	1.758	0.963	5	13.443	2.989	3	2.700	0.850	2	13.443
Mo98	0.046	0.021	5	0.063	0.005	3	0.130	0.080	2	0.130
Ni60	0.576	0.264	5	1.603	0.454	3	0.605	0.455	2	1.603
Pb208	0.075	0.060	5	3.317	3.426	3	0.215	0.135	2	3.317
Se82	2.112	1.245	5	2.437	1.177	3	2.185	0.715	2	2.437
Sn	4.990	1.352	5	57.493	60.993	3	12.340	6.860	2	57.493
Sr88	6.912	9.346	5	330.537	71.845	3	7.500	2.680	2	330.537
U238	0.003	0.002	5	0.020	0.006	3	0.009	0.007	2	0.020
Zn64	17.074	7.870	5	49.940	8.841	3	33.660	0.160	2	49.940

Muscle tissue, typically considered a major site for TE bioaccumulation in many organisms, showed the highest concentration for only one element, arsenic, which may reflect species-specific metabolic pathways or storage patterns.

Significant differences were detected for 7 out of 15 TEs (Table S5), emphasizing that TE distribution varies considerably between tissues. Dunn’s post hoc analysis further narrowed these findings, confirming significant inter-tissue differences for 6 elements (Cu, Fe, Mn, Pb, Sr, and Zn). These results indicate that skin and muscle tissues are most differentiated in their TE concentrations (Figure 6), suggesting skin as a prominent site for certain metals like zinc and lead, which could be linked to external accumulation or

binding in the dermal layer. The $\epsilon 2$ highlights a large size effect for 4 out of 15 TEs: Co, Mn, Sr, and Zn.

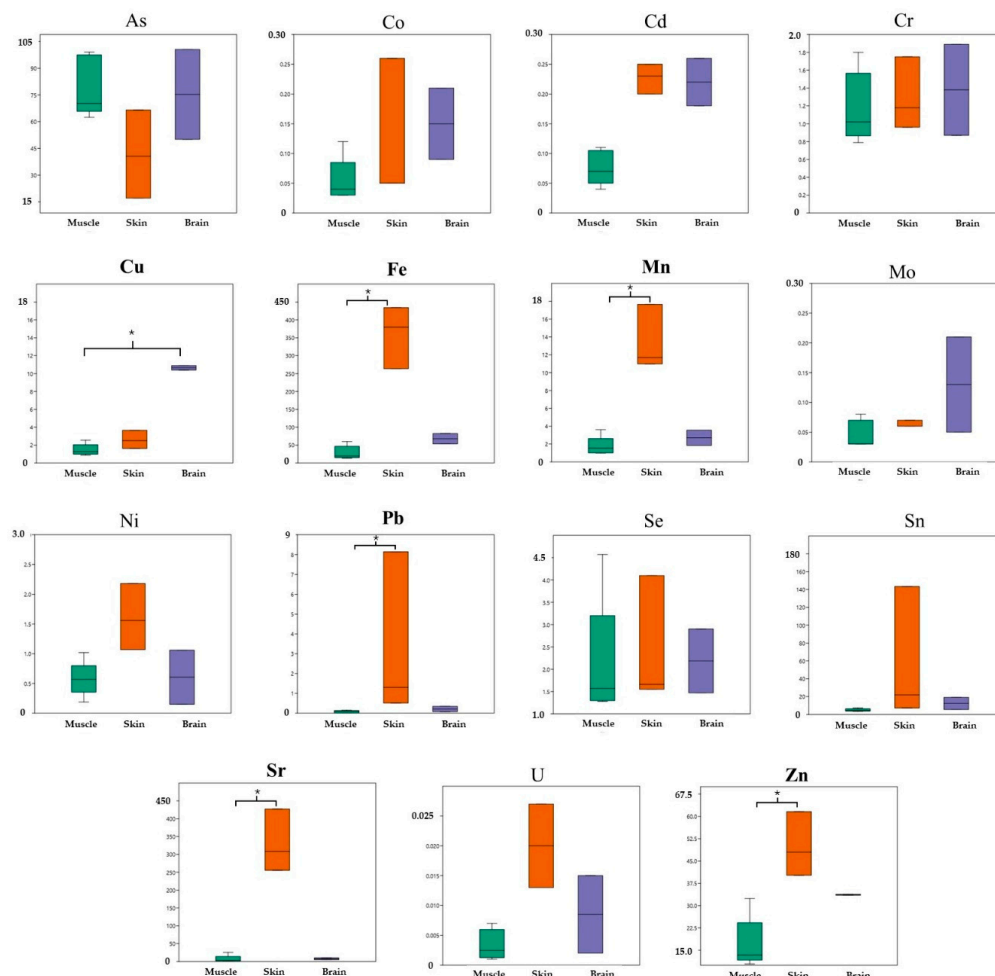


Figure 6. Kruskal–Wallis and Dunn’s post hoc tests performed for tissue. The figure includes box plots (with standard deviation) for all 15 elements. Elements showing significant differences are highlighted in bold. The figure also shows the species that exhibited significant differences according to Bonferroni correction during Dunn’s post hoc test, as follows: $p \leq 0.05$ (*). On the X-axis, the different tissues analyzed are represented, while on the Y-axis, the concentration is reported relative to dry weight and expressed in ppm (mg/kg).

The unique case of Cu showed significant differences between the brain and muscle, highlighting the potential for copper’s neurological roles or specific regulatory mechanisms within brain tissue. This points to tissue-specific bioaccumulation and regulatory processes that align with the distinct functions and exposure levels of different organs. It is interesting to note that higher levels of Cd correspond to lower levels of Zn, a known antagonistic effect described in the literature [44].

4. Conclusions

This study provides critical insights into how dietary habits, trophic levels, metabolic pathways, and environmental exposure influence trace element (TE) bioaccumulation in elasmobranchs. The results highlight significant interspecies and inter-trophic-level differences, suggesting that ecological and physiological factors jointly shape these patterns. Elements such as aluminum, barium, and selenium demonstrated strong positive correlations with trophic level, underscoring the central role of diet in their accumulation. In contrast, negative correlations observed for elements like cobalt and manganese point to

active metabolic regulation or excretion processes. Interestingly, elements such as arsenic and lead showed no correlation with trophic levels, indicating that localized environmental contamination or specific detoxification pathways likely contribute to their variability, further emphasizing the multifaceted nature of TE bioaccumulation.

Tissue-specific accumulation patterns revealed the skin as a major site for TE deposition, reflecting its direct environmental exposure and barrier functions. Muscle and brain tissues displayed distinct accumulation trends, driven by their unique metabolic roles. For example, elevated copper levels in the brain align with its essential neurological functions, while antagonistic interactions between cadmium and zinc illustrate the complexity of metal interactions within tissues. These findings provide a nuanced understanding of how different tissues manage metal exposure and underscore the protective or essential physiological mechanisms at play.

The observed accumulation of toxic elements such as lead and nickel in endangered species, including *Hexanchus griseus* and *Prionace glauca*, raises significant conservation concerns. These results suggest potential long-term health risks for these species and highlight their value as sentinel indicators for marine contamination. Moreover, the findings have implications for human health, particularly in regions where these species are consumed as seafood, underscoring the need for careful monitoring of contamination levels.

Overall, this study emphasizes the critical role of elasmobranchs in assessing marine pollution, given their trophic position and ecological significance. To build on these findings, future research should expand the scope of species and geographic regions analyzed, investigate the influence of environmental factors on TE dynamics, and explore the physiological mechanisms underpinning metal accumulation and detoxification. These efforts will not only enhance our understanding of TE bioaccumulation but also inform conservation strategies and pollution mitigation measures, ultimately contributing to the sustainable management of marine ecosystems.

Supplementary Materials: The following supporting information can be downloaded at: <https://www.mdpi.com/article/10.3390/environments12010012/s1>, Table S1: Raw data obtained from the analysis of the muscle tissue in the 12 species for the 16 TEs.; Table S2: Results of the Kruskal–Wallis test and ϵ^2 in the comparison among species (five), with KW values and p values; Table S3: Results of the Kruskal–Wallis test and ϵ^2 in the comparison among trophic levels (six), with KW values and p values; Table S4: Raw data obtained from the analysis of three tissues in *G. melastomus* for the 15 TEs; Table S5: Results of the Kruskal–Wallis test and ϵ^2 in the comparison among tissues (three), with KW values and p values.

Author Contributions: Conceptualization, E.S., D.B., M.B., S.I. and C.M.; methodology, D.B., S.G., G.G., E.S. and C.M.; formal analysis, S.G., E.S., G.G., F.L.L. and D.B.; investigation, F.R.R., P.M., L.P., S.G., G.G. and F.L.L.; resources, M.B., D.B., E.S., C.M., P.M. and S.I.; data curation, S.G., F.R.R., G.G., F.L.L. and L.P.; writing—original draft preparation, S.G., D.B., M.B. and E.S.; writing—review and editing, D.B., P.M., G.G., F.L.L., S.I., M.B., F.R.R. and C.M.; supervision, E.S., D.B., M.B. and P.M.; funding acquisition, M.B., E.S., D.B., S.I. and C.M. All authors have read and agreed to the published version of the manuscript.

Funding: This research was funded by “Fondo per lo sviluppo e la coesione (FSC) - Centro Ricerche ed Infrastrutture Marine Avanzate in Calabria (CRIMAC) - CUP C64I20000320001”.

Institutional Review Board Statement: The chondrichthyan specimens enrolled in the present work were obtained from commercial fisheries or stranding events. The activity was conducted under the conditions of the Regulation of the European Parliament and the Council for fishing in the General Fisheries Commission for the Mediterranean (GFCM) Agreement area and amended Council Regulation (EC) No. 1967/2006. All procedures were carried out with the approval of the “Ministero della transizione ecologica—MiTE” (n. authorization 0008263, 25 January 2022).

Informed Consent Statement: Not applicable.

Data Availability Statement: Data are available on request due to restrictions, e.g., privacy or ethical.

Acknowledgments: Authors are grateful to Paola Fittipaldi, Raffaella Santoro, Sandro Tripepi, Pina Cacciola and Carlo De Donato for their help during samples processing.

Conflicts of Interest: The authors declare no conflicts of interest.

References

1. Consales, G.; Marsili, L. Assessment of the Conservation Status of Chondrichthyans: Underestimation of the Pollution Threat. *Eur. Zool. J.* **2021**, *88*, 165–180. [[CrossRef](#)]
2. Storelli, M.M.; Marcotrigiano, G.O. Interspecific Variation in Total Arsenic Body Concentrations in Elasmobranch Fish from the Mediterranean Sea. *Mar. Pollut. Bull.* **2004**, *48*, 1145–1149. [[CrossRef](#)]
3. Storelli, M.M.; Giacomini-Stuffler, R.; Marcotrigiano, G. Mercury Accumulation and Speciation in Muscle Tissue of Different Species of Sharks from Mediterranean Sea, Italy. *Bull. Environ. Contam. Toxicol.* **2002**, *68*, 201–210. [[CrossRef](#)] [[PubMed](#)]
4. Storelli, M.M. Potential Human Health Risks from Metals (Hg, Cd, and Pb) and Polychlorinated Biphenyls (PCBs) via Seafood Consumption: Estimation of Target Hazard Quotients (THQs) and Toxic Equivalents (TEQs). *Food Chem. Toxicol.* **2008**, *46*, 2782–2788. [[CrossRef](#)] [[PubMed](#)]
5. Alves, L.M.F.; Nunes, M.; Marchand, P.; Le Bizec, B.; Mendes, S.; Correia, J.P.S.; Lemos, M.F.L.; Novais, S.C. Blue Sharks (*Prionace glauca*) as Bioindicators of Pollution and Health in the Atlantic Ocean: Contamination Levels and Biochemical Stress Responses. *Sci. Total Environ.* **2016**, *563–564*, 282–292. [[CrossRef](#)] [[PubMed](#)]
6. Barrera-García, A.; O'Hara, T.; Galván-Magaña, F.; Méndez-Rodríguez, L.C.; Castellini, J.M.; Zenteno-Savín, T. Trace Elements and Oxidative Stress Indicators in the Liver and Kidney of the Blue Shark (*Prionace glauca*). *Comp. Biochem. Physiol. A. Mol. Integr. Physiol.* **2013**, *165*, 483–490. [[CrossRef](#)] [[PubMed](#)]
7. Canli, M.; Atli, G. The Relationships between Heavy Metal (Cd, Cr, Cu, Fe, Pb, Zn) Levels and the Size of Six Mediterranean Fish Species. *Environ. Pollut.* **2003**, *121*, 129–136. [[CrossRef](#)]
8. De Boeck, G.; Eyckmans, M.; Lardon, I.; Bobbaers, R.; Sinha, A.K.; Blust, R. Metal Accumulation and Metallothionein Induction in the Spotted Dogfish *Scyliorhinus canicula*. *Comp. Biochem. Physiol. A Mol. Integr. Physiol.* **2010**, *155*, 503–508. [[CrossRef](#)] [[PubMed](#)]
9. Jeffree, R.A.; Warnau, M.; Teyssié, J.-L.; Markich, S.J. Comparison of the Bioaccumulation from Seawater and Depuration of Heavy Metals and Radionuclides in the Spotted Dogfish *Scyliorhinus canicula* (Chondrichthys) and the Turbot *Psetta maxima* (Actinopterygii: Teleostei). *Sci. Total Environ.* **2006**, *368*, 839–852. [[CrossRef](#)]
10. Lopez, S.A.; Abarca, N.L.; Meléndez, R.C. Heavy Metal Concentrations of Two Highly Migratory Sharks (*Prionace glauca* and *Isurus oxyrinchus*) in the Southeastern Pacific Waters: Comments on Public Health and Conservation. *Trop. Conserv. Sci.* **2013**, *6*, 126–137. [[CrossRef](#)]
11. Merly, L.; Lange, L.; Meyer, M.; Hewitt, A.M.; Koen, P.; Fischer, C.; Muller, J.; Schilack, V.; Wentzel, M.; Hammerschlag, N. Blood Plasma Levels of Heavy Metals and Trace Elements in White Sharks (*Carcharodon carcharias*) and Potential Health Consequences. *Mar. Pollut. Bull.* **2019**, *142*, 85–92. [[CrossRef](#)] [[PubMed](#)]
12. Barrera-García, A.; O'Hara, T.; Galván-Magaña, F.; Méndez-Rodríguez, L.C.; Castellini, J.M.; Zenteno-Savín, T. Oxidative Stress Indicators and Trace Elements in the Blue Shark (*Prionace glauca*) off the East Coast of the Mexican Pacific Ocean. *Comp. Biochem. Physiol. Part C Toxicol. Pharmacol.* **2012**, *156*, 59–66. [[CrossRef](#)]
13. Marcovecchio, J.E.; Moreno, V.J.; Pérez, A. Metal Accumulation in Tissues of Sharks from the Bahía Blanca Estuary, Argentina. *Mar. Environ. Res.* **1991**, *31*, 263–274. [[CrossRef](#)]
14. Vas, P. Trace Metal Levels in Sharks from British and Atlantic Waters. *Mar. Pollut. Bull.* **1991**, *22*, 67–72. [[CrossRef](#)]
15. Torres, P.; Da Cunha, R.T.; Maia, R.; Dos Santos Rodrigues, A. Trophic Ecology and Bioindicator Potential of the North Atlantic Tope Shark. *Sci. Total Environ.* **2014**, *481*, 574–581. [[CrossRef](#)]
16. Torres, P.; Tristão Da Cunha, R.; Micaelo, C.; Rodrigues, A.D.S. Bioaccumulation of Metals and PCBs in *Raja clavata*. *Sci. Total Environ.* **2016**, *573*, 1021–1030. [[CrossRef](#)]
17. McKinney, M.A.; Dean, K.; Hussey, N.E.; Cliff, G.; Wintner, S.P.; Dudley, S.F.J.; Zungu, M.P.; Fisk, A.T. Global versus Local Causes and Health Implications of High Mercury Concentrations in Sharks from the East Coast of South Africa. *Sci. Total Environ.* **2016**, *541*, 176–183. [[CrossRef](#)]
18. Bevacqua, L.; Reinero, F.R.; Becerril-García, E.E.; Elorriaga-Verplancken, F.R.; Juaristi-Videgaray, D.; Micarelli, P.; Galván-Magaña, F.; Curiel-Godoy, P.; Giglio, G.; Tripepi, S.; et al. Trace Elements and Isotopes Analyses on Historical Samples of White Sharks from the Mediterranean Sea. *Eur. Zool. J.* **2021**, *88*, 132–141. [[CrossRef](#)]
19. Pethybridge, H.; Cossa, D.; Butler, E.C.V. Mercury in 16 Demersal Sharks from Southeast Australia: Biotic and Abiotic Sources of Variation and Consumer Health Implications. *Mar. Environ. Res.* **2010**, *69*, 18–26. [[CrossRef](#)]

20. Matulik, A.G.; Kerstetter, D.W.; Hammerschlag, N.; Divoll, T.; Hammerschmidt, C.R.; Evers, D.C. Bioaccumulation and Biomagnification of Mercury and Methylmercury in Four Sympatric Coastal Sharks in a Protected Subtropical Lagoon. *Mar. Pollut. Bull.* **2017**, *116*, 357–364. [[CrossRef](#)] [[PubMed](#)]
21. Bendall, V.A.; Barber, J.L.; Papachlitzou, A.; Bolam, T.; Warford, L.; Hetherington, S.J.; Silva, J.F.; McCully, S.R.; Losada, S.; Maes, T.; et al. Organohalogen Contaminants and Trace Metals in North-East Atlantic Porbeagle Shark (*Lamna nasus*). *Mar. Pollut. Bull.* **2014**, *85*, 280–286. [[CrossRef](#)] [[PubMed](#)]
22. Taylor, D.L.; Kutil, N.J.; Malek, A.J.; Collie, J.S. Mercury Bioaccumulation in Cartilaginous Fishes from Southern New England Coastal Waters: Contamination from a Trophic Ecology and Human Health Perspective. *Mar. Environ. Res.* **2014**, *99*, 20–33. [[CrossRef](#)] [[PubMed](#)]
23. Filice, M.; Reinero, F.R.; Cerra, M.C.; Faggio, C.; Leonetti, F.L.; Micarelli, P.; Giglio, G.; Sperone, E.; Barca, D.; Imbrogno, S. Contamination by Trace Elements and Oxidative Stress in the Skeletal Muscle of Scyliorhinus canicula from the Central Tyrrhenian Sea. *Antioxidants* **2023**, *12*, 524. [[CrossRef](#)]
24. Storelli, M.M.; Cuttone, G.; Marcotrigiano, G.O. Distribution of Trace Elements in the Tissues of Smooth Hound *Mustelus mustelus* (Linnaeus, 1758) from the Southern–Eastern Waters of Mediterranean Sea (Italy). *Environ. Monit. Assess.* **2011**, *174*, 271–281. [[CrossRef](#)] [[PubMed](#)]
25. Reinero, F.R.; Milazzo, C.; Minervino, M.; Marchio, C.; Filice, M.; Bevacqua, L.; Giglio, G.; Leonetti, F.L.; Micarelli, P.; Tripepi, S.; et al. Parasitic Load, Hematological Parameters, and Trace Elements Accumulation in the Lesser Spotted Dogfish *Scyliorhinus canicula* from the Central Tyrrhenian Sea. *Biology* **2022**, *11*, 663. [[CrossRef](#)] [[PubMed](#)]
26. The IUCN Red List of Threatened Species. Available online: <https://www.iucnredlist.org/en> (accessed on 3 December 2024).
27. Sperone, E.; Parise, G.; Leone, A.; Milazzo, C.; Circosta, V.; Santoro, G.; Paolillo, G.; Micarelli, P.; Tripepi, S. Spatiotemporal Patterns of Distribution of Large Predatory Sharks in Calabria (Central Mediterranean, Southern Italy). *Acta Adriat.* **2012**, *53*, 13–24.
28. Ebert, D.A.; Sarah, F. *Sharks of the World: A Complete Guide*; Princeton University Press: Princeton, NJ, USA, 2021; Volume 19.
29. Gallo, S.; Nania, G.; Caruso, V.; Zicarelli, G.; Leonetti, F.L.; Giglio, G.; Fedele, G.; Romano, C.; Bottaro, M.; Mangoni, O.; et al. Bioaccumulation of Trace Elements in the Muscle of the Blackmouth Catshark *Galeus melastomus* from Mediterranean Waters. *Biology* **2023**, *12*, 951. [[CrossRef](#)]
30. De Donato, C.; Barca, D.; Milazzo, C.; Santoro, R.; Giglio, G.; Tripepi, S.; Sperone, E. Is Trace Element Concentration Correlated to Parasite Abundance? A Case Study in a Population of the Green Frog *Pelophylax synkl. hispanicus* from the Neto River (Calabria, Southern Italy). *Parasitol. Res.* **2017**, *116*, 1745–1753. [[CrossRef](#)]
31. Cortes, E. Standardized Diet Compositions and Trophic Levels of Sharks. *ICES J. Mar. Sci.* **1999**, *56*, 707–717. [[CrossRef](#)]
32. Jacobsen, I.P.; Bennett, M.B. A Comparative Analysis of Feeding and Trophic Level Ecology in Stingrays (Rajiformes; Myliobatoidei) and Electric Rays (Rajiformes: Torpedinoidei). *PLoS ONE* **2013**, *8*, e71348. [[CrossRef](#)] [[PubMed](#)]
33. Gaion, A.; Scuderi, A.; Sartori, D.; Pellegrini, D.; Ligas, A. Trace Metals in Tissues of *Galeus melastomus* Rafinesque, 1810 from the Northern Tyrrhenian Sea (NW Mediterranean). *Acta Adriat.* **2016**, *57*, 165–172.
34. Roubie, E.; Karavoltos, S.; Sakellari, A.; Katsikatsos, N.; Dassenakis, M.; Megalofonou, P. Trace Metals Distribution in Tissues of 10 Different Shark Species from the Eastern Mediterranean Sea. *Fishes* **2024**, *9*, 77. [[CrossRef](#)]
35. Hornung, H.; Krom, M.D.; Cohen, Y.; Bernhard, M. Trace Metal Content in Deep-Water Sharks from the Eastern Mediterranean Sea. *Mar. Biol.* **1993**, *115*, 331–338. [[CrossRef](#)]
36. LeBlanc, P.J.; Jackson, A.L. Arsenic in Marine Fish and Invertebrates. *Mar. Pollut. Bull.* **1973**, *4*, 88–90. [[CrossRef](#)]
37. Giovos, I.; Brundo, M.V.; Doumpas, N.; Kazlari, Z.; Loukovitis, D.; Moutopoulos, D.K.; Spyridopoulou, R.N.A.; Papadopoulou, A.; Papapetrou, M.; Tiralongo, F. Trace Elements in Edible Tissues of Elasmobranchs from the North Aegean Sea (Eastern Mediterranean) and Potential Risks from Consumption. *Mar. Pollut. Bull.* **2022**, *184*, 114129. [[CrossRef](#)] [[PubMed](#)]
38. Torres, P.; Tristão Da Cunha, R.; Rodrigues, A.D.S. Mid-Atlantic Elasmobranchs: Suitable Metal Scouts? *Mar. Pollut. Bull.* **2017**, *117*, 203–213. [[CrossRef](#)] [[PubMed](#)]
39. Hauser-Davis, R.A.; Rocha, R.C.C.; Saint’Pierre, T.D.; Adams, D.H. Metal Concentrations and Metallothionein Metal Detoxification in Blue Sharks, *Prionace glauca* L. from the Western North Atlantic Ocean. *J. Trace Elem. Med. Biol.* **2021**, *68*, 126813. [[CrossRef](#)] [[PubMed](#)]
40. Álvaro-Berlanga, S.; Calatayud-Pavía, C.E.; Cruz-Ramírez, A.; Soto-Jiménez, M.F.; Liñán-Cabello, M.A. Trace Elements in Muscle Tissue of Three Commercial Shark Species: *Prionace glauca*, *Carcharhinus falciformis*, and *Alopias pelagicus* off the Manzanillo, Colima Coast, Mexico. *Environ. Sci. Pollut. Res.* **2021**, *28*, 22679–22692. [[CrossRef](#)]
41. Mille, T.; Cresson, P.; Chouvelon, T.; Bustamante, P.; Brach-Papa, C.; Bruzac, S.; Rozuel, E.; Bouchoucha, M. Trace Metal Concentrations in the Muscle of Seven Marine Species: Comparison between the Gulf of Lions (North-West Mediterranean Sea) and the Bay of Biscay (North-East Atlantic Ocean). *Mar. Pollut. Bull.* **2018**, *135*, 9–16. [[CrossRef](#)]

42. Kiszka, J.J.; Aubail, A.; Hussey, N.E.; Heithaus, M.R.; Caurant, F.; Bustamante, P. Plasticity of Trophic Interactions among Sharks from the Oceanic South-Western Indian Ocean Revealed by Stable Isotope and Mercury Analyses. *Deep Sea Res. Part Oceanogr. Res. Pap.* **2015**, *96*, 49–58. [[CrossRef](#)]
43. Nussey, G.; van Vuren, J.; du Preez, H.H. Bioaccumulation of Chromium, Manganese, Nickel and Lead in the Tissues of the Moggel, *Labeo umbratus* (Cyprinidae), from Witbank Dam, Mpumalanga. *Water SA* **2000**, *26*, 269–284.
44. Brzóska, M.M.; Moniuszko-Jakoniuk, J. Interactions between Cadmium and Zinc in the Organism. *Food Chem. Toxicol.* **2001**, *39*, 967–980. [[CrossRef](#)]

Disclaimer/Publisher’s Note: The statements, opinions and data contained in all publications are solely those of the individual author(s) and contributor(s) and not of MDPI and/or the editor(s). MDPI and/or the editor(s) disclaim responsibility for any injury to people or property resulting from any ideas, methods, instructions or products referred to in the content.